Modeling Phenol Degradation in a Fluidized-Bed Bioreactor

A study was made of phenol degradation by bacteria immobilized onto particles of calcined diatomaceous earth in a draft-tube, three-phase fluidized-bed reactor.

A mathematical model is used to describe simultaneous diffusion and reaction of oxygen and phenol in the reactor. Kinetic parameters for the growth of nonsupported cells were obtained in batch and chemostat experiments. Liquid-solid mass transfer coefficients were determined experimentally and showed good agreement with literature values for conventional three-phase fluidized beds. Experimental steady-state degradation data were used to calculate biofilm substrate diffusivities. These were found to decrease as the biofilm density increased.

The transition from phenol to oxygen-limiting biofilm kinetics predicted by the model was shown to exist experimentally. A critical ratio of phenol/dissolved oxygen concentration was found at which this transition occurred. This provides a criterion for establishing whether increased aeration will increase the volumetric degradation rate.

Andrew G. Livingston
Howard A. Chase
Department of Chemical Engineering
University of Cambridge
Cambridge CB2 3RA, England

Introduction

Biological films are commonly used in waste water treatment (trickle filter, rotating disk) as they provide several advantages over freely-suspended cell systems. These include high biomass concentration, increased resistance to toxic shock loadings (Parkin and Spence, 1984), and higher volumetric throughputs due to the independence of cell growth rate from reactor dilution rate. Holladay et al. (1978) and Denac and Dunn (1987) have compared packed- vs. fluidized-bed biofilm reactors containing immobilized microorganisms and found the fluidized-bed reactor to be more efficient in terms of volumetric degradation capacity. Fan et al. (1987) have showed that the performance for phenol degradation of a three-phase fluidized-bed reactor fitted with a draft tube to promote the internal circulation of the liquid and solid phases is superior to that of a conventional three-phase fluidized bed.

In this work a three-phase fluidized-bed reactor (FBR) with an internal draft tube is used to study the biodegradation of phenol, mass transfer from the bulk liquid to the bioparticle, and diffusion and reaction within the bioparticle. An ion exchange resin is used to determine the liquid-solid mass transfer coefficient. A mixed microbial culture attaches itself to the solid support particles by natural adsorption. The support particles used are Celite R-632, a calcined diatomaceous earth produced by Manville Corp., U.S.A. Steady states are established in the FBR and a mathematical model is used to calculate the relative diffusivities and effectiveness factors in the biofilm.

Previous workers in this field (Tang and Fan, 1987; Worden and Donaldson, 1987) have proposed models describing mass transfer and reaction in these types of reactors, but the range of experimental validation of these models is limited to the case when one substrate controls the reaction rate. In the present work, conditions are varied so that the limiting substrate undergoes a transition from phenol to oxygen. This allows the verification of the two-substrate-limiting kinetic expression and establishes a criterion for determining whether the degradation rate is oxygen- or phenol-limited.

Mathematical Model

A model describing the microbial degradation of phenol by immobilized bacteria was developed along similar lines to the one employed by Tang and Fan (1987). Liquid-solid mass transfer was accounted for using mass transfer coefficients. Two substrates, phenol and oxygen, were assumed to be simultaneously diffusing into and reacting within the biofilm. Monod kinetics for oxygen, coupled with a Haldane-type expression for the

Correspondence concerning this paper should be addressed to A. G. Livingston.

inhibitory effects of phenol, were used to describe microbial growth.

There are three basic processes occurring in the biodegradation of phenol in a FBR:

a) Transport of oxygen from the gas phase into the bulk liquid.

b) Transport of phenol, oxygen and other nutrients from the bulk liquid phase to the surface of the biofilm.

c) Simultaneous diffusion and reaction of phenol, oxygen and other nutrients within the biofilm.

Process (a) was not considered in this work as the concentration of dissolved oxygen in the liquid phase was held constant by adding oxygen to either nitrogen or air in the inlet gas as required.

A pseudosteady state was assumed to exist in the FBR when the concentrations of oxygen and phenol in the liquid phase and the biomass loading on the support particles were constant over a 24-hour period. Under these conditions, the concentration profiles of oxygen and phenol across the liquid film and within the biofilm were assumed to be constant with respect to time. The following assumptions were made in the development of the model:

1. The FBR can be approximated as a completely-mixed system. This assumption is reasonable in view of the recirculation of the liquid and solid phases in the reactor. An experiment using a pulse of dilute HCl as a tracer and monitoring the pH showed that the reactor contents circulated completely every 6 seconds, and that the pulse was completely mixed with the reactor contents after 30 seconds. The response time of the pH electrode was measured as being less than 1 second.

2. Particle-particle and particle-wall collisions, together with fluid turbulence, shear excess biomass off the solid particles so that an equilibrium is reached between the growth rate of biomass and the removal rate of biomass. It is this equilibrium that is assumed to maintain the biomass loading constant at pseudosteady state. The validity of this assumption can be tested by comparing the difference in phenol concentration between the inlet and outlet streams with the amount of biomass produced. If the assumption is valid, the amount of biomass produced should be equal to the phenol consumed multiplied by the yield coefficient for biomass on phenol. This was difficult to do experimentally as the biomass in the reactor effluent was present not as freely-suspended cells but as flocs which had been sheared off the bioparticles. These tended to settle in the overflow from the reactor, making the determination of the biomass content in the reactor effluent problematic. However, approximate measurements showed a good agreement (within 20–30%).

3. The "free" cells sloughed off the bioparticles make only a negligible contribution to the overall degradation rate. This seems reasonable in view of the relative holdup of immobilized biomass in the reactor being typically in the range 2–4 kg · m^{-3} compared to the holdup of suspended biomass which was in the range of 0.040–0.080 kg · m^{-3} and also the fact that the reactor was being operated at a dilution rate approximately six times greater than μ_{max} of the cells.

4. The Celite particles were assumed to be spherical and the average particle diameter was used in all calculations involving the particle size.

5. The biomass forms an even coating on the outside surface of the Celite particles: i.e., the cell growth within the pores is insignificant (electron microscopy showed no cells growing in the interior of the particles), and the biofilm is a homogeneous phase.

6. The growth-limiting nutrients are phenol and oxygen. All other nutrients are present in excess. The growth kinetics are assumed to follow Monod kinetics with respect to oxygen and substrate-inhibited kinetics with respect to phenol. The expression for the specific growth rate as a function of substrate concentrations is thus:

$$\mu = \frac{\mu_{max} S}{(S + K_s + S^2/K_i)} \frac{C}{(C + K_o)} \tag{1}$$

The consumption of substrates for cell maintenance energy is assumed to be insignificant.

7. Immobilization of the cells into the biofilm does not change the kinetic parameters describing the rate of growth: i.e., Eq. 1 describes growth of free or immobilized cells equally well and with the same constants.

8. The ratio of D_{of}/D_{ow} is the same as the ratio D_{sf}/D_{so}: i.e., the diffusivities of oxygen and phenol are reduced to the same extent in the biofilm.

9. The Celite remains totally inert during all experiments and does not adsorb phenol.

Under the above assumptions, a mass balance for phenol over the FBR can be written:

$$R_{sobs} = Q(S_I - S_b) \tag{2}$$

A mass balance over a thin shell of the biofilm leads to the following equations describing the concentration profiles of phenol and oxygen, respectively:

$$D_{sf}\left[\frac{d^2S}{dr^2} + \frac{2}{r}\left(\frac{dS}{dr}\right)\right] = \frac{\rho_v}{Y_{x/s}} \frac{\mu_{max} S}{(S + K_s + S^2/K_i)} \frac{C}{(C + K_o)} \tag{3}$$

$$D_{of}\left[\frac{d^2C}{dr^2} + \frac{2}{r}\left(\frac{dC}{dr}\right)\right] = \frac{\rho_v}{Y_{x/o}} \frac{\mu_{max} S}{(S + K_s + S^2/K_i)} \frac{C}{(C + K_o)} \tag{4}$$

The corresponding boundary conditions for these equations are:

$$\left(\frac{dS}{dr}\right) = \left(\frac{dC}{dr}\right) = 0 \quad \text{at} \quad r = r_p \tag{5}$$

$$D_{sf}\left(\frac{dS}{dr}\right) = k_s (S_b - S_i) \quad \text{at} \quad r = r_p + \delta \tag{6}$$

$$D_{of}\left(\frac{dC}{dr}\right) = k_o (C_b - C_i) \quad \text{at} \quad r = r_p + \delta \tag{7}$$

Equations 2–7 can be rewritten in terms of dimensionless variables as follows:

$$\frac{d^2S^*}{dx^2} + \frac{2}{(x + r_p/\delta)} \frac{dS^*}{dx} = \phi_s \frac{S^*}{(S^* + K_S^* + S^{*2} K_i^*)} \frac{C^*}{(C^* + K_o^*)} \tag{8}$$

$$\frac{d^2C^*}{dx^2} + \frac{2}{(x + r_p/\delta)} \frac{dC^*}{dx} = \phi_o \frac{S^*}{(S^* + K_S^* + S^{*2} K_i^*)} \frac{C^*}{(C + K_o^*)} \tag{9}$$

$$\frac{dS^*}{dx} = \frac{dC^*}{dx} = 0 \quad \text{at} \quad x = 0.0 \tag{10}$$

$$\frac{dS^*}{dx} = Bi_s (1 - S^*) \quad \text{at} \quad x = 1.0 \tag{11}$$

$$\frac{dC^*}{dx} = Bi_o (1 - C^*) \quad \text{at} \quad x = 1.0 \tag{12}$$

where

$$S^* = \frac{S}{S_b} \quad C^* = \frac{C}{C_b} \quad x = \frac{r - r_p}{\delta} \quad K_s^* = \frac{K_s}{S_b} \quad K_i^* = \frac{S_b}{K_i}$$

$$K_o^* = \frac{K_o}{C_b} \qquad \phi_s = \frac{\rho_v \mu_{max} \delta^2}{Y_{x/s} D_{sf} S_b} \qquad \phi_o = \frac{\rho_v \mu_{max} \delta^2}{Y_{x/o} D_{of} C_b}$$

$$Bi_s = \frac{k_s \delta}{D_{sf}} \qquad Bi_o = \frac{k_o \delta}{D_{of}}$$

The phenol degradation rate can be found after Eq. 8-12 have been solved by integrating the reaction rate over the biofilm for a single bioparticle and multiplying by the number of particles in the reactor, e.g.

$$R_{scalc} = \frac{N_p \rho_v}{Y_{x/s}} \int_{r-r_p}^{r-r_p+\delta} \cdot \frac{\mu_{max} S}{(S + K_s + S^2/K_i)} \frac{C}{(C + K_o)} 4\pi r^2 dr \tag{13}$$

This is equivalent to calculating the flux at the surface of the bioparticles, e.g.

$$R_{scalc} = A_p k_s (S_b - S_i) = A_p D_{sf} \left(\frac{dS}{dr}\right)_{r-r_p+\delta} \tag{14}$$

where

$$A_p = N_p 4\pi (r_p + \delta)^2$$

Thus two *values* can be arrived at for the overall phenol degradation rate:

1. R_{sobs} is given by Eq. 2.
2. R_{scalc} is given by solving Eq. 8-12 and using the resulting concentration profiles to obtain R_{scalc} via Eq. 13.

With two values for the phenol degradation rate, one or more of the system parameters can be adjusted until the two rates are in agreement. Two approaches have been used in different parts of this work:

Method A: finding the relative diffusivity, D_f/D_w, from the experimental data

In an experiment S_b and C_b are measured and fixed at their respective steady-state values. The actual phenol degradation rate is then given by Eq. 2, R_{sobs}. The diffusivities of oxygen and phenol are adjusted relative to their values in water, until the values of R_{scalc}, obtained by solving Eq. 8-12 followed by Eq. 13, agrees with R_{sobs}.

Method B: predicting phenol concentration assuming fixed C_b and known D_f/D_w

Assuming the values of C_b and D_f/D_w are known, it is possible to find, by solving Eq. 2 and 8-13 iteratively, a value for S_b which makes both phenol degradation rates, R_{sobs} and R_{scalc}, equal. This value can then be compared to the experimentally-measured value.

Numerical methods

Equations 8-12 comprise a nonlinear, boundary value problem. This was solved using the method of orthogonal collocation (Villadsen and Michelson, 1978; Finlayson, 1980). The set of nonlinear equations for S^* and C^* at the collocation points were solved using a National Algorithims Group (NAG) (U.K. Ltd) routine C05NBF. This routine uses a modification of the Powell hybrid method (Powell, 1970). An accuracy of 5.0×10^{-5} was specified for the solution of these equations. A continuation facility was included to obtain the initial solution. Iterations were performed until the calculated and observed rates of phenol degradation agreed to within 0.1%.

Experimental Materials and Methods

Microbial culture and inoculum

Three strains of bacteria reported to be capable of utilizing phenol as the sole carbon and energy source were obtained from the National Collection of Industrial Bacteria (U.K.) Ltd. These were NCIB 8250 (*Acineobacter sp.*), NCIB 10535 (*Pseudomonas sp.*), and NCIB 1015 (*Pseudomonas sp.*). These strains were revived from freeze-dried samples and stored on agar plates containing 50 mg · L^{-1} phenol. An inoculum was prepared from these stored samples by growing a loop of each in 100 mL of growth medium overnight or until all phenol had been metabolized. The samples were then mixed together and used to inoculate the FBR.

Growth medium

The growth medium used had the constituents listed in Table 1, made up to volume using tap water. Sterile conditions were not maintained in this work. Concentrated phenol was added to the medium as it flowed to the reactor to provide a synthetic wastewater with a phenol concentration between 65.0 and 132.0 mg · L^{-1}.

Matrix for cell immobilization

The solid matrix to which the microbes attached themselves by natural adsorption was a calcined diatomaceous earth, Celite R-632 produced by Manville Corp. (U.S.A.). This chemically-inert matrix consists of diatomaceous earth diatoms which are broken up and then recalcined to give controlled pore sizes and particle diameters. The chemistry of microbial adhesion to surfaces is as yet not very well understood; however, previous work has shown that Celite particles are suitable for immobilizing a

Table 1. Growth Medium

Constituent	Conc. mg·L^{-1}
Potassium Dihydrogen Orthophosphate KH_2PO_4	420
Dipotassium Hydrogen Orthophosphate K_2HPO_4	375
Ammonium Sulfate $(NH_4)_2SO_4$	244
Sodium Chloride NaCl	15
Calcium Chloride $CaCl_2$	15
Magnesium Sulfate $MgSO_4$	30
Ferrous Chloride $FeCl_2$	2

wide range of microbes (Caunt and Chase, 1988; Wang et al., 1984; Robinson et al., 1985; Baker et al., 1984). The Celite particles were sieved on a mechanical vibrator for 20 minutes, and the size fraction between 750 and 1180 $\times 10^{-6}$ m was kept and used herein. Before addition to the FBR, the Celite was washed with tap water to remove fines and dust generated during handling.

Phenol assay

Phenol concentrations were measured using gas chromatography. A Philips PU 4000 chromatograph was fitted with a 1.52-m-long 4-mm-ID glass column packed with Porapack P (mesh range 80–100). The carrier gas flow rate was set at 45 mL/min, which gave a sample analysis time of less than 7 minutes. By using sample volumes of up to 10 μL, phenol concentrations down to 1.0 mg · L^{-1} could be detected with an error of 0.25 mg · L^{-1}. Samples were withdrawn from the FBR using a syringe and then filtered immediately through a 0.22-μm filter unit to remove any microbes present in the sample which would decrease the phenol concentration by their degradative activity. The peak on the chromatogram corresponding to phenol was found to be symmetrical, and a linear relationship between peak height and phenol concentration was established using calibration samples of known concentration.

Determination of biomass loading and biofilm thickness

The biomass loading in terms of the mass of dry biomass per unit mass of Celite support was measured as follows: a sample of biomass-laden particles (0.5–1.5 mL) was withdrawn from the FBR and washed with 100 mL of distilled water to remove any unattached biomass and any metal salts that could upset the latter stages of the procedure by giving up their water of crystallization. This sample was then transferred to a weighed sample vial and placed in an oven at 110°C for at least 16 hours to remove all unbound moisture. The sample vial was then weighed and placed in a furnace at 600°C for 2 hours to burn off all the biomass present, followed by reweighing. The biomass loading was calculated as the difference between the two weighings divided by the total weight of Celite present in the sample. No correction was made for ash content. Duplicate samples were taken for each determination and were found to vary usually by less than 10%. Typical samples contained around 0.1 g of Celite, and the average weight of Celite particle was determined from the mean of over 200 particle weights as $m_p = 1.713 \times 10^{-4}$ g, giving around 600 particles in each sample. A control sample showed that the process did not affect the Celite particles.

The biofilm thickness was determined by measuring the mean diameter of a sample of over 50 bioparticles removed from the FBR on an Optomax V (Analytical Instruments Ltd, U.K.) image analyzer. The video input was from a microscope, and the individual particle diameters were measured by equating the projected area on the analyzer screen to the diameter of a sphere which would project an equal area. The sample was then dried and placed in a furnace at 600°C to burn off the biomass and the diameter remeasured. Measurements before and after biomass removal were carried out with the particles under a constant depth of water to negate any lens effects. The biofilm thickness was calculated as half the difference in diameters between the biomass-laden sample and the biomass-free sample. A series of control experiments were conducted to test the error of this method of determining particle diameter, which was found to average approximately 8×10^{-6} m.

Determination of kinetic parameters

The kinetic parameters describing the growth of the unsupported microbial culture on phenol were determined from batch growth experiments. A range of initial phenol concentrations (from 20.0 to 500.0 mg · L^{-1}) were used as initial concentrations in 250-mL shake flasks containing 95 mL of medium. An inoculum for use in these experiments was obtained by growing microbes present in the FBR effluent overnight in a growth medium containing initially 100.0 mg · L^{-1} phenol. Five mL of this inoculum was added to each of the shake flasks which were incubated on a Gallenkamp orbital incubator at 30°C and 200 rpm. The optical absorbance of the culture at 660 nm was measured at 40–50 minute intervals, and the specific growth rate determined from the slope of a plot of $\log_e$ (optical absorbance) against time.

Determination of yield coefficients

The yield coefficients for growth of the microorganisms on phenol were determined in a chemostat culture. A 1-L L.H. Fermentation (U.K. Ltd.) Series 500 turbine-agitated fermenter was used at dilution rates of 0.227 to 0.636 h^{-1} and an inlet phenol concentration of 200.0 to 220.0 mg · L^{-1}. To start each run, approximately 100 mL of settled microbial flocs were taken from the outlet of the FBR and added to 900 mL of medium. Air flow was set to $2.67-3.33 \times 10^{-6}$ $m^3 \cdot s^{-1}$. This was sufficient to maintain the dissolved oxygen concentration above 4.5 mg · L^{-1}. The temperature was held at 30°C and the pH controlled to between 6.7 and 6.9 by corrective addition of 1M HCl or 1M NaOH. After the passage of a minimum of six fermenter volumes of liquid, steady state was assumed to have been reached and measurements of biomass and phenol concentration in the fermenter medium were made. Biomass concentration in the chemostat was determined by filtering a 50-mL sample through a preweighed 0.22-μm filter paper. The paper was dried at 110°C and the dry weight of biomass in the sample determined by reweighing. Oxygen concentration in the offgas was measured using a Sybron Taylor paramagnetic oxygen analyzer. The gas flow rate and the change in oxygen concentration between the inlet and outlet streams could thus be used to calculate the rate of oxygen uptake.

Fluidized-bed reactor

Equipment. A diagram of the FBR is shown in Figure 1. The reactor had a volume of 1,200 mL, was constructed from perspex, and consisted of a 50-mm-ID reaction zone 1,680-mm-high fitted with a 29-mm-ID draft tube 660-mm-high. A 70-mm-ID, 80-mm-high solid-liquid separation zone at the top of the reactor had an angled effluent discharge so that solids entrained by gas bubbles escaping around the base of the baffle and rising through the separation zone were not washed out of the reactor. The pH was controlled as in the yield coefficient experiments to between 6.7 and 6.9, and the temperature was held at 30°C. The dissolved oxygen was measured with a galvanic-type probe and controlled if desired by addition of oxygen to either air or nitrogen, with the pressures regulated so that the overall gas flow remained constant. Gas entered at the base of the FBR via a Grade P40 (B.D.H., U.K. Ltd.) sintered glass gas

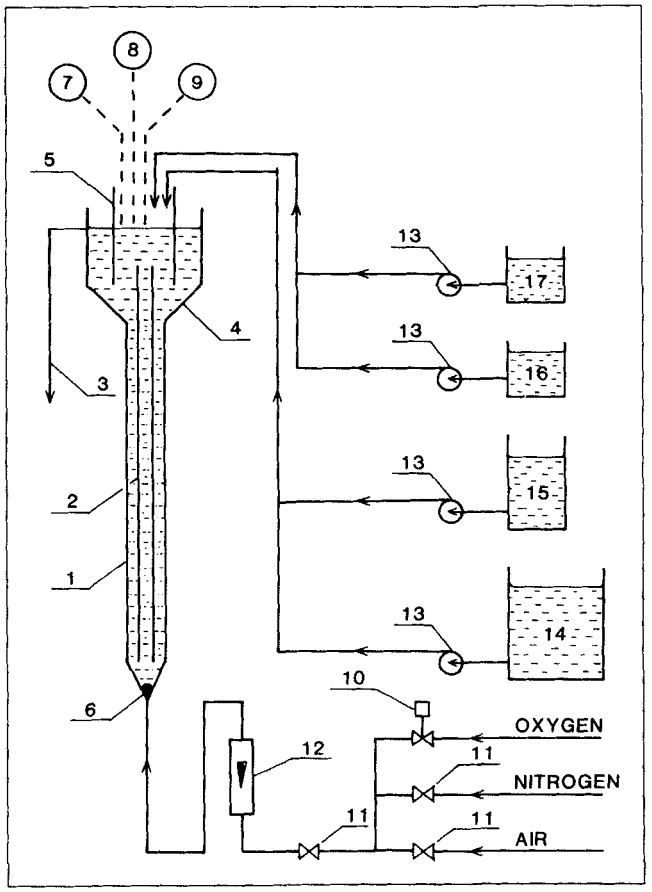

Figure 1. Fluidized-bed reactor.

(1) Draft Tube Fluidized Bed Reactor
(2) Draft Tube
(3) Effluent Overflow
(4) Solid-Liquid Disengagement Zone
(5) Baffle
(6) Sintered Glass Gas Distribution Tube
(7) Temperature Controller
(8) pH Controller
(9) Dissolved Oxygen Controller
(10) Solenoid Valve
(11) Gas Flow Control Valves
(12) Gas Flow Meter
(13) Peristaltic Pump
(14) Growth Medium
(15) Concentrated Phenol Solution
(16) Acid
(17) Alkali

distribution tube which had a pore size range of 16 to 40 μm. In all experiments, the gas flow was high enough so that the reactor was operating in circulating solids mode, i.e., at gas velocities which were sufficient to create circulation of solids and liquid between the draft and annular regions. The recirculating liquid flow was typically of the order of 600 reactor volumes per hour. The feed flow rate was typically two to four reactor volumes per hour. Thus the recirculating flow ensured no short circuiting took place between the feed and the overflow.

Start-Up of the FBR. 300–400 mL of inoculum were added to 800–900 mL of medium in the FBR. The phenol concentration was bought up to 200 mg · L^{-1} by the addition of concentrated phenol solution, and the system run in batch mode until all the phenol had been utilized. Operation was switched to continuous with a dilution rate of 0.15–0.25 h^{-1} and a feed concentration of 200.0 mg · L^{-1} for a period of approximately 24 hours to allow the microbial population to stabilize. Celite was then added to the reactor and the system left for 4–5 days to allow the growth of a biofilm before experiments were begun.

Steady-State Phenol Degradation in the FBR. Pseudosteady-state conditions were assumed to exist in the system when the phenol concentration, biomass loading, and biofilm thickness remained constant over a 24–36-hour period. Five such steady states were established, and the conditions prevailing in each are given in Table 2. The volume fraction of bioparticles in all these runs was 9.75%.

Effect of Dissolved Oxygen Concentration on FBR Performance. In these runs the oxygen concentration was varied to evaluate its effect on the phenol degradation rate with a constant phenol load applied to the FBR. Starting with the steady-state dissolved oxygen concentration obtained with air flowing through the reactor, the gas flow was switched from air to nitrogen as required: i.e., when the desired setpoint for oxygen concentration was below the concentration established using air, the main gas was changed to nitrogen and oxygen dosed into the gas stream to control the dissolved oxygen at the desired level. Phenol concentration was assayed every 15 minutes to determine when the new steady state had been obtained.

Liquid solid mass transfer coefficient

For the mathematical model to be successfully applied, knowledge of the liquid-solid mass transfer coefficients for phenol and oxygen is required. The mass transfer coefficients were measured using an ion exchange resin following the method of Sanger and Dewcker (1981). Ion exchange processes involving beads of ion exchange resin in a packed bed or suspended in a liquid can be rate limited by liquid-solid mass transfer, diffusion within the beads, or the reaction kinetics of the ion exchange process itself. Helfferich (1962) provides the following dimensionless group to determine whether the main resistance to ion exchange is in the mass transfer step or internal diffusion:

$$\alpha = \frac{XD_i\lambda 2}{cD_e d_p}\left(5 + \frac{2}{K_{ba}}\right) \tag{15}$$

The system Na^+/H^+ was used in this work, and we can calculate the value of α, assuming $D_e = 1.33 \times 10^{-9}$ $m^2 \cdot s^{-1}$ (Atkins, 1986), as: $D_i = 4.5 \times 10^{-11}$ $m^2 \cdot s^{-1}$ (Helfferich, 1962); $K_{ba} = 1.2$ (Bauman and Eichorn, 1947); $X = 1.9$ mol · L^{-1} (trade literature); $c = 0.0001$ mol · L^{-1}; $\lambda = 0.1 \times 10^{-4}$ m; and $d_p = 9.25 \times 10^{-4}$ m (measured). This gives $\alpha = 93$. Thus, since $\alpha \gg 1$ for the system and conditions used herein, mass transfer is the rate-limiting step, and the rate of concentration change of ions in the

Table 2. Steady-State Conditions

Steady-State No.	Liquid Flow ($m^3 \cdot s^{-1}$) $\times 10^7$	Gas Flow ($m^3 \cdot s^{-1}$) $\times 10^6$	S_i ($kg \cdot m^{-3}$) $\times 10^3$	C_b ($kg \cdot m^{-3}$) $\times 10^3$
1	9.07	15.0	82.7	4.69
2	10.23	15.0	92.3	4.24
3	8.65	15.0	131.7	4.54
4	9.22	15.0	108.5	5.58
5	9.38	15.0	83.0	6.25

bulk liquid can be written as:

$$-\frac{dc}{dt} = k_e a(c - c_i) \tag{16}$$

This expression can be integrated to give:

$$\ln\frac{c - c_i}{c_o - c_i} = -k_e a\Delta t \tag{17}$$

During the early stages of the ion exchange, the concentration at the surface of the resin bead is negligible (i.e., $c_i = 0$) and:

$$k_e = \frac{2.303}{a}\frac{\Delta pH}{\Delta t} \tag{18}$$

where a is calculated from:

$$a = \frac{6\epsilon_p}{d_p} \tag{19}$$

ϵ_p was assumed to be equal to 0.65 of the settled volume of the resin divided by the reactor volume. Thus the liquid-solid mass transfer coefficient could be calculated from a knowledge of the initial slope of the pH vs. time curve when a pulse of dilute HCl was injected into the FBR.

The gas flow rate in the FBR during the mass transfer experiments was the same as that used during the steady-state runs, i.e., 15×10^{-6} m$^3 \cdot$ s^{-1}, which gives $u_g = 0.903 \times 10^{-2}$ m $\cdot$ s^{-1}. Dowex 50-X8 (Na^+ form) ion exchange resin beads were allowed to swell and then size fractionated by settling in water to give a narrower size distribution (The original size distribution of the beads was 0.3–1.15 mm). The particle size of a sample of 100 of these fractionated beads was measured using the Optomax V. A measured volume of beads (90 or 180 mL) was added to distilled water in the FBR. The pH at the start of each run varied between 6.6 and 5.0. A pulse of 10 mL of dilute HCl was added to the FBR over a 12-second interval to counter the effect of the liquid circulation producing oscillations in the pH reading. The pH was monitored and the initial slope of the pH versus time curve evaluated from a chart recorder trace. The experiment was performed at least 3 times at each of the two solids loadings.

Results and Discussion

Liquid-solid mass transfer coefficient: experimental values vs. correlation for a conventional FBR

The results of the experiments performed to establish k_e are given in Table 3. The particle diameter d_p of the ion exchange resin was found to be 925.0×10^{-6} m with a standard deviation of 187.0×10^{-6} m. It is assumed that the effect of the size distribution is not significant. The mass transfer coefficient was independent of the solids volume fraction over the range tested.

Table 3. Results of Mass Transfer Experiments

Vol. Frac. Resin Beads	a (m^2/m^3)	$\Delta pH/\Delta t$ s^{-1}	k_e ($m \cdot s^{-1}$)
5.0%	316.0	0.023 ± 0.001	1.67×10^{-4}
10.0%	732.0	0.046 ± 0.009	1.67×10^{-4}

No correlations have been published for the liquid-solid mass transfer coefficient in a FBR equipped with a draft tube. Tang et al. (1987) performed a single experiment using beads of benzoic acid in a draft tube FBR and found close agreement between their measured value of k_s and a value obtained from a correlation published by Arters and Fan (1986) for a conventional FBR. In order to compare the mass transfer coefficient determined herein with correlated values for conventional FBR's, the interdiffusion coefficient for the Na^+/H^+ system was calculated according to Helfferich (1962) as:

$$D_{12} = \frac{2D_1D_2}{D_1 + D_2} \tag{20}$$

The correlation given by Arters and Fan is:

$$Sh = (2.0 + 0.695Sc^{0.33})\left(\frac{\epsilon d_p^4}{v}\right)^{0.2} \tag{21}$$

where ϵ is calculated from

$$\epsilon = u_g g \tag{22}$$

This correlation predicted a mass transfer coefficient of 1.4×10^{-4} m $\cdot$ s^{-1} for the Na^+/H^+ system, which is in reasonable agreement with the value of 1.7×10^{-4} obtained experimentally. The specific gravity of the ion exchange resin is approximately 1.23. The specific gravity of the bioparticles was determined by measuring the settling velocities of 50 particles which had a biomass loading of 0.110 kg $\cdot$ kg^{-1}, and using the relationship between drag coefficient and Reynolds Number found by Lapple and Sheppard (1940) and given in Perry (1984) to calculate the particle density, ρ_p, which gave $\rho_p = 1.157$. It was thus assumed that the slip velocity and fluid mechanical environment surrounding the two types of particles were similar. Thus the correlation (Eq. 21) was used to predict the mass transfer coefficients of phenol and oxygen, giving $k_s = 0.66 \times 10^{-4}$ m $\cdot$ s^{-1} and $k_o = 1.37 \times 10^{-4}$ m $\cdot$ s^{-1}.

Kinetic parameters of microbial growth

The specific growth rate in each shake flask was determined by plotting graphs of $\log_e$ (optical absorbance) against time over the initial period of cell growth. Small inoculums were used so that the substrate concentration could be assumed constant in this initial growth period. This assumption was tested by monitoring the phenol concentration using absorbance at 270 nm as a direct "quick" test. Although inaccurate at concentrations of phenol under 10.0 mg $\cdot$ L^{-1}, it was used to ensure that all points used in the logarithmic plots were derived from samples taken at times when the phenol concentration was at least 70% of the initial value. The variation of μ with S obtained from these experiments is shown in Figure 2.

The Haldane equation for substrate-inhibited growth was fitted to the data of μ as a function of S using a nonlinear least squares technique (NAG routine E04 FDF). The data yielded the following parameters: $\mu_{max} = 0.418$ h^{-1} (1.161×10^{-4}s^{-1}); $K_s = 2.9$ mg $\cdot$ L^{-1} (0.0029 kg $\cdot$ m^{-3}); $K_i = 370.0$ mg $\cdot$ L^{-1} (0.370 kg $\cdot$ m^{-3}). These values agree reasonably well with the values obtained by Yang and Humphrey (1975) ($K_s = 2.38$, $K_i = 106.0$ mg $\cdot$ L^{-1}) and Hill et al. (1975)

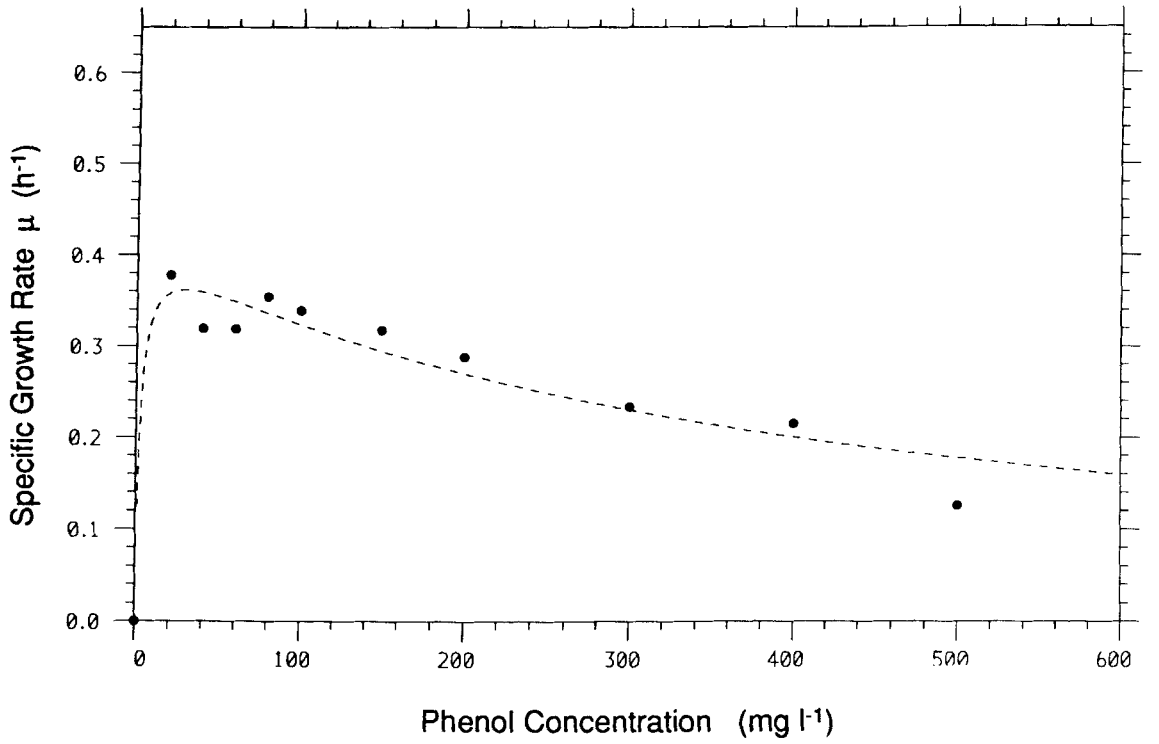

Figure 2. Results of shake flask experiments to determine cell growth parameters at 30°C.

(●) Experimental data; (-----) haldane substrate inhibition function fitted via least squares. The parameters obtained are: μ_{max} = 0.418 h^{-1}; K_s = 2.29 mg · L^{-1}; K_i = 370.0 mg · L^{-1}

($K_s < 1.0$, $K_i = 470.0$ mg · L^{-1}), for the growth of *Pseudomonas putida* on phenol at 30°C.

When using a nonsterile system which is inoculated with three different microbial strains and operated as a continuous culture it is likely that the microbial population will be a mixed culture. Thus it is difficult to make a valid direct comparison of the kinetic parameters obtained in this study with those obtained in another. The effect of the value of K_i is minimal on the results calculated below as the substrate concentrations do not reach high enough levels to cause any significant inhibitory effects in any of the steady states established. K_s, on the other hand, has a marked effect on the calculated concentration profiles in the biofilm. For example, for steady-state run 2 a 20% variation in K_s from the experimentally-determined value of 2.29 mg · L^{-1} causes a 13% variation in the calculated value of the relative diffusivity. However, since the inoculums used in the shake flask experiments were taken from the FBR reactor itself, the parameters obtained from these experiments are assumed to be the best estimates and are used in all the following calculations.

The value of the Monod constant for oxygen, K_o, was not determined in this study. This parameter becomes important when the phenol degradation rate is limited by the oxygen concentration. Atkinson and Mavituna (1983) list values of K_o for microorganisms in the range of 0.4–0.0001 mg · L^{-1}. Recently Wagner and Hempel (1988) have experimentally determined the K_o for *Pseudomonas sp.* A3 growing on napthalene sulfonate as 2.6 mg · L^{-1} at 30°C. Since napthalene sulfonate and phenol are both aromatic compounds, and *Pseudomonas* bacteria were used in both studies, a value of 0.26 mg · L^{-1} (0.26×10^{-3} kg · m^{-3}) has been assumed in this work.

The experiments to determine yield coefficients used the chemostat. The value of $Y_{x/s}$ obtained in this work was $Y_{x/s}$ = 0.60 + 0.12 kg biomass · kg phenol $^{-1}$. This agrees well with $Y_{x/s}$ values reported in the literature for microorganisms growing on phenol [Hill et al. (1975), 0.52; Palowsky and Howell (1973), 0.545–0.616; Yang and Humphrey (1975), 0.585]. The value of $Y_{o/s}$ was 1.29 ± 0.16 kg oxygen · kg phenol^{-1}. This is in good agreement with the values obtained by Tang and Fan (1987) of 1.4 and Klein et al. (1979) of 1.36. The value of $Y_{x/o}$ was obtained by dividing $Y_{x/s}$ by $Y_{o/s}$ to give 0.465 kg biomass · kg oxygen^{-1}. Assumption 6, in which cell maintenance is negligible, is validated by the results for the yield coefficients at varying dilution rates, which indicated no apparent correlation between yield and dilution rate. Wall growth was observed in some of the chemostat runs, but no correction was made for this effect. The maximum stable dilution rate reached was 0.636 h^{-1}, which is somewhat in excess of the μ_{max} for the culture of 0.418 h^{-1}. This discrepancy is attributed to the presence of immobilized cells in the fermenter as a result of wall growth.

Steady-state phenol degradation: relative diffusivity of substrates in the biofilm

The experimental data gathered for the five steady state runs are shown in Table 4. The biofilm dry density is calculated from:

$$\rho_v = \frac{L\, m_p}{4/3\pi\, [(r_p + \delta)^3 - r_p^3]} \tag{23}$$

where r_p is the radius of the biomass-free Celite particles averaged over all the samples, found to be 509.0×10^{-6} m. The val-

Table 4. Steady-State Runs

Run No.	S_b kg·m^{-3} × 10^3	S_i kg·m^{-3} × 10^3	L kg·kg^{-1} × 10^3	δ m × 10^6	ρ_v kg·m^{-3}	D_f/D_w	Bi_s	θ
1	2.55	1.17	64.9	23.1	141.3	0.88	1.98	0.475
2	4.05	2.33	85.3	22.1	194.5	0.30	5.76	0.306
3	12.02	10.07	105.6	24.4	217.0	0.05	34.46	0.178
4	5.84	4.07	116.7	26.2	222.6	0.12	17.24	0.181
5	3.79	2.40	114.5	26.2	218.5	0.16	12.26	0.179

ues of D_f/D_w and S_i/S_b were calculated following Method A outlined previously. D_{sw} and D_{ow} are taken as 0.87×10^{-9} and 2.54×10^{-9} m^2 · s^{-1} at 30°C, respectively (Washburn, 1926).

The calculated concentration profiles in the biofilm for run 2 are shown in Figure 3. It can be seen from this figure that the concentration of phenol approaches zero at the surface of the Celite particle ($x = 0.0$), while the concentration of oxygen reaches a steady finite value. In this particular run, phenol can be considered as limiting the reaction rate. This was true for all the runs except run 3, which was limited by oxygen.

The values of ρ_v lie in a similar range to those obtained by Tang and Fan (1987) for bacteria growing on activated carbon particles in a similar reactor (70–151 kg · m^{-3}). In the initial start-up period of the FBR, a lower gas flow rate of 11×10^{-6} m^3 · s^{-1} was used. A bulky, fibrous biofilm with trailing tendrils was observed to grow until a biomass loading of 0.154 kg · kg^{-1} was reached. At this point the gas flow rate was increased to 20×10^{-6} m^3 · s^{-1} for a period of 3 days, after which the biomass loading had decreased to 0.04 kg · kg^{-1}. The biofilms at this stage were observed to be smooth. The gas flow rate was then set to the value of 15×10^{-6} m^3 · s^{-1} used during the steady-state runs. Thus it would seem that the nature of the biofilm and its density depend heavily on the conditions of shear in the FBR. Formation of a smooth dense biofilm is favored by turbulent conditions.

It can be seen from the values of S_i in Table 4 that the liquid-solid mass transfer accounts for a large portion of the transport resistance. The effect is less marked at higher biofilm densities which have lower relative diffusivities, D_f/D_w. The Biot number for a species gives an indication of the relative importance of diffusion vs. reaction. The Biot number for phenol, Bi_s, is listed in Table 4. It ranges from 2.0 to 34.3. This indicates that the mass transfer resistance is important in limiting the overall rate of reaction. In several previous models proposed for diffusion and reaction in biofilms, the liquid-solid mass transfer has been assumed to be negligible (Andrews and Chi-Tien, 1981; Park et al., 1984; Wang and Chi-Tien, 1984; Worden and Donaldson, 1987). The results of this work would suggest that this assumption may lead to significant errors.

Much work has been done on estimating the diffusivity of oxygen and other substrates in microbial films and flocs. A summary of this work using microbial aggregates has recently been

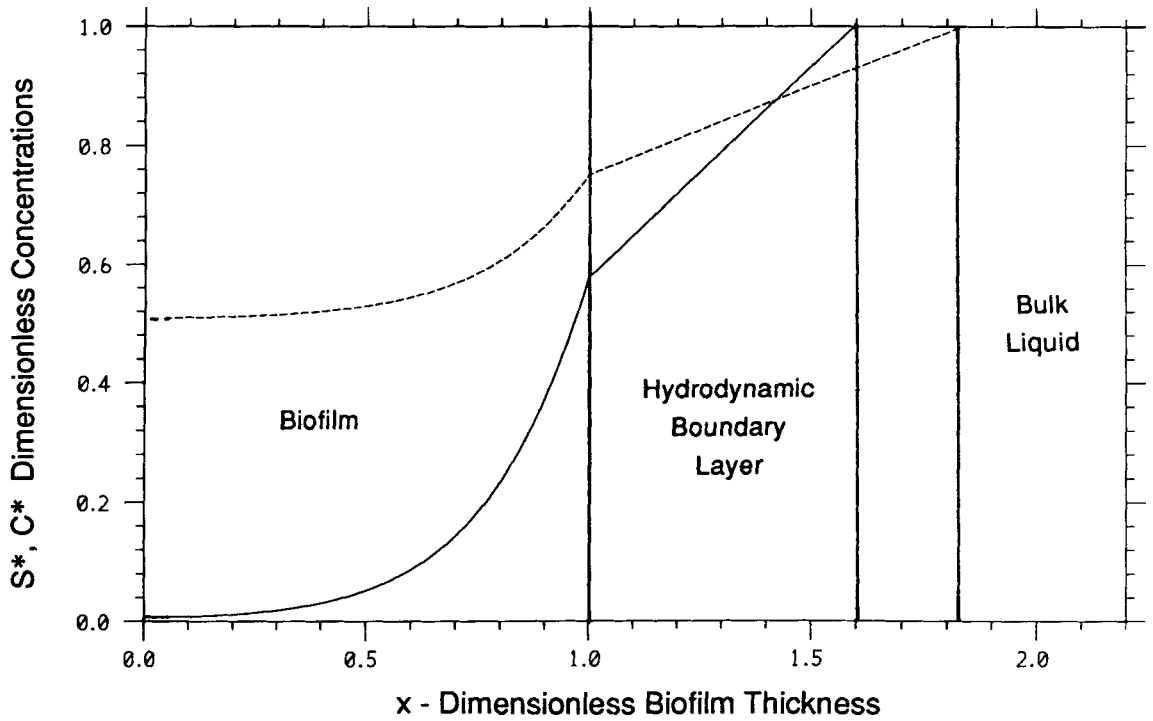

Figure 3. Calculated concentration profile in the biofilm for steady-state run 2 (——) S* (----) C*.
Hydrodynamic boundary layer thickness has been calculated as k/D_w.

made by Libicki et al. (1988). The diffusivity has been found to vary from between 2% to over 100% of the value in water with a number of diffusing species. It would appear that the relative diffusivity D_f/D_w is a function of the thickness and density of the microbial aggregates. Figure 4 shows D_f/D_w plotted against the biofilm density. As the density of the biofilm increases D_f/D_w decreases from a value of 0.88 to approximately 0.05.

Libicki et al. (1988) used an inert tracer in a living biofilm to determine D_f/D_w as the cell volume fraction varies from 0 to 1 and found it decreased from 1.0 to around 0.25. The data collected do not allow the cell volume fraction for the biofilms to be determined, but although a direct compairson of the data cannot be made, the results agree qualitatively. Tang and Fan (1987) found that in a system comprising an FBR and a mixed microbial culture grown on activated carbon particles, D_f/D_w ranged from 0.245 to 0.086 as ρ_v varied from 72 to 151 kg · m^{-3}. The results of this work are thus in good agreement with other studies.

A standard way of comparing the relative importance of diffusion and reaction is to define an effectiveness factor, θ where

$$\theta = \frac{\text{actual rate of reaction}}{\text{rate of reaction with no diffusional limitation}}$$

in this case θ can be shown to be:

$$\theta = \frac{Q\,(S_I - S_b)}{\dfrac{W}{Y_{x/s}}\dfrac{\mu_{\max} S_i}{S_i + K_s + S_i^2/K_i}\dfrac{C_i}{C_i + K_o}} \tag{24}$$

The calculated values of θ are given in Table 4. A plot of θ vs. ρ_v is shown in Figure 4. As the biofilm density increases from 140.0 to 220.0 the effectiveness factor decreases from a value near 0.5 to a value of 0.18. This result is to be expected as higher biofilm densities on the particles lead to lower diffusion coefficients in the biofilm as discussed above. This increases the role biofilm diffusion plays in limiting the reaction rate.

Effect of dissolved oxygen concentration on the phenol degradation rate: experiment vs. theory

In several studies of fluidized-bed biofilm reactors for the degradation of phenol it has been noted that increasing the dissolved oxygen concentration results in an increase in the degradation rate (Donaldson et al., 1984; Worden and Donaldson, 1987). Tang and Fan (1987) found that the phenol degradation rate was independent of the dissolved oxygen concentration over the range of conditions used in their work. The purpose of this section was to determine experimentally the interdependence of S_b and C_b at given phenol loading rates ($Q \cdot S_I$) and to compare the results with theoretically-obtained values.

It was found that, with the FBR running in an initial steady state, when the dissolved oxygen concentration was altered a new steady state was established within 40–60 minutes. Figure 5 shows the measured phenol concentration varying as the dissolved oxygen level is altered. Thus conditions could be varied so that several steady state S_b, C_b combinations could be determined over a period of several hours. The biofilm properties (L, ρ_v) were measured at the beginning and end of the series of experiments and found to be constant. Plots of S_b vs. C_b at two different phenol loadings are shown in Figures 6a and 6b.

As the oxygen concentration in the bulk liquid is decreased, there is an initial range over which the phenol concentration is unaffected. This region corresponds to phenol being the limiting substrate in the biofilm, and Eqs. 3 and 4 can effectively be written:

$$\frac{d^2S}{dr^2} + \frac{2}{r}\frac{dS}{dr} = \frac{\rho_v}{Y_{x/s}}\frac{\mu_{\max} S}{(S + K_s)} \tag{25}$$

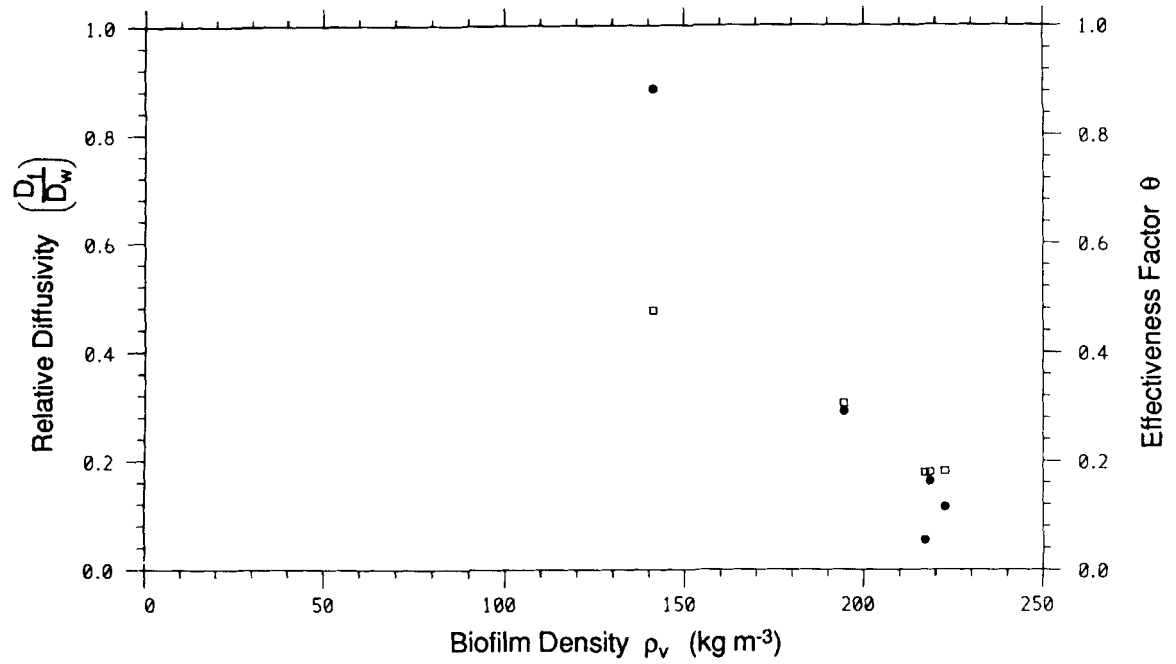

Figure 4. Relative diffusivity D_f/D_w (●) and effectiveness factor θ (□) as a function of biofilm density ρ_v.
Experimental data have been fitted by a mathematical model to calculate D_f for oxygen and phenol. The effectiveness factor is defined in Eq. 24.

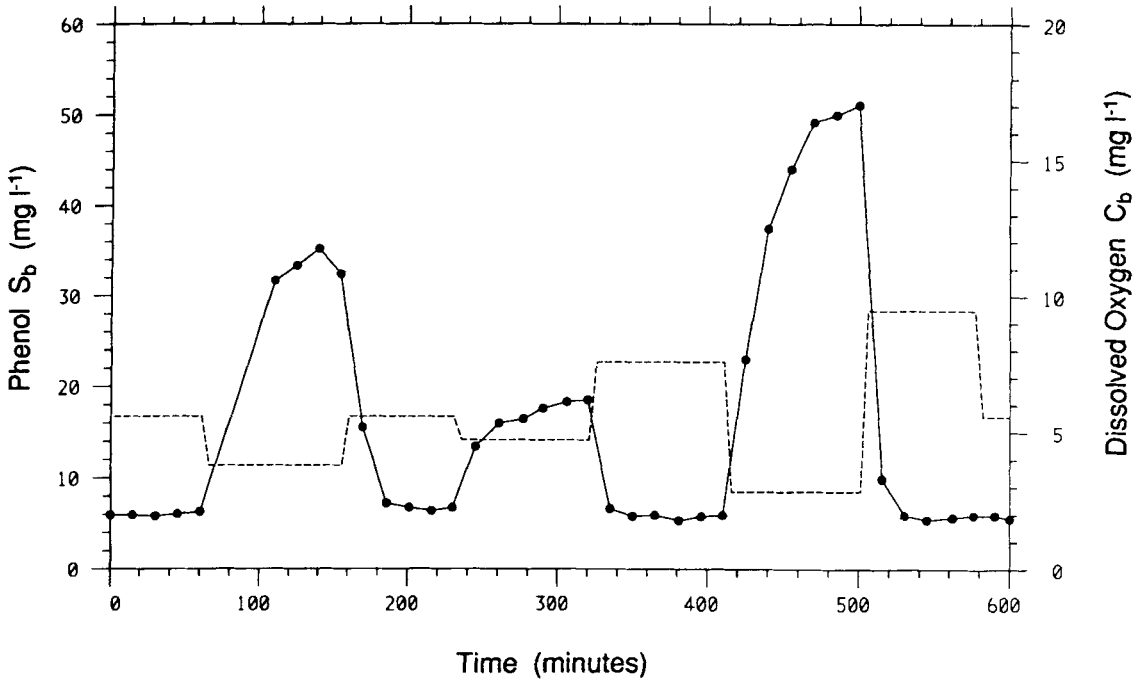

Figure 5. Response of measured phenol concentration S_b (●) to controlled dissolved oxygen concentrations C_b (----).
Phenol loading rate ($Q \cdot S_l$) = 1.0×10^{-7} kg · s^{-1}. Flow rate, $Q = 9.22 \times 10^{-7}$ m^3 · s^{-1}.

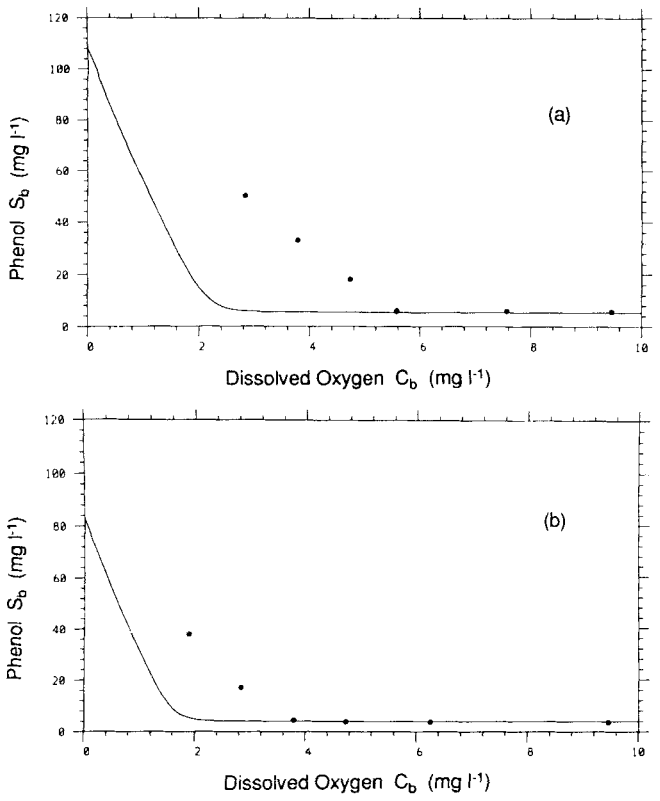

Figure 6. Phenol concentration as a function of dissolved oxygen concentration at fixed phenol loading rates $Q \cdot S_l$.
(●) Experimental data (——); theoretically-predicted curve with parameters as listed in Table 5.
(a) $Q \cdot S_l = 1.0 \times 10^{-7}$ *kg* · *s*$^{-1}$
(b) $Q \cdot S_l = 0.78 \times 10^{-7}$ *kg* · *s*$^{-1}$

$$\frac{d^2C}{dr^2} + \frac{2}{r}\frac{dC}{dr} = \frac{\rho_v}{Y_{x/o}} \frac{\mu_{\max} S}{(S + K_s)} \tag{26}$$

since the reaction is zero-order w.r.t. oxygen ($C_b \gg K_o$) and the inhibitory effect of phenol is not important ($S_b \ll K_i$). As C_b is progressively decreased, the rate of reaction changes from being limited by phenol concentration to being limited by the dissolved oxygen concentration. However, the rate of reaction is not zero order with respect to phenol because, while $S_b \gg K_s$, the inhibition term S^2/K_i becomes increasingly important. The flow rates of gas and liquid for these two runs, Figures 6a and 6b, are the same as those for steady states 4 and 5, respectively and are listed in Table 2.

The theoretical curves shown in Figures 6a and 6b were calculated using Method B given previously and assuming the parameter values listed in Table 5. They are seen to be in reasonable agreement with the experimental data. One reason why the theoretical curves do not give a better agreement could be that the value of the Monod constant for oxygen, K_o, obtained from the literature and assumed to apply to this study, could be inaccurate. Figure 7 shows the effect of varying K_o on the theoretically-determined curves. The parameter values are the same as those listed in Table 5 except for K_o, which is as given. It would seem from this figure that a value of K_o higher than 0.26 mg · L^{-1} (0.26×10^{-3} kg · m^{-3}) gives better agreement between the experimental data and theory. More experimental work is required to determine K_o specifically for this sytem and to verify that a better fit can be obtained using independently-determined values of K_o. It is, however, encouraging to note that the transition predicted by the dual substrate-limiting kinetic model has in fact been verified experimentally.

A cricital value of S_b/C_b was found to exist for the transition from oxygen-limited to phenol-limited biofilm kinetics. At values above the critical ratio, S_b increased rapidly as C_b decreased,

Table 5. Model Parameters for Figures 6 and 7

Parameter	Value	Units
D_{of}	0.356×10^{-9}	$m^2 s^{-1}$
D_{sf}	0.125×10^{-9}	$m^2 s^{-1}$
μ_{max}	1.161×10^{-4}	s^{-1}
K_s	2.9×10^{-3}	$kg \cdot m^{-3}$
K_i	370.0×10^{-3}	$kg \cdot m^{-3}$
K_o	0.26×10^{-3}	$kg \cdot m^{-3}$
$Y_{x/s}$	0.6	$kg \cdot kg^{-1}$
$Y_{x/o}$	0.465	$kg \cdot kg^{-1}$
k_s	0.66×10^{-4}	$m \cdot s^{-1}$
k_o	1.37×10^{-4}	$m \cdot s^{-1}$
N_p	2.245×10^{5}	—
r_p	509.0×10^{-6}	m
δ	26.1×10^{-6}	m
ρ_v	6a–222.6	
	6b & 7–218.5	$kg \cdot m^{-3}$

while below the critical ratio changes in C_b left S_b unaffected (Figures 6 and 7). This critical ratio was found experimentally to be in the range of 0.9–1.1. Donaldson et al. (1984) used pure oxygen to maintain C_b at 1 to 2 mg · L^{-1} and noted that using air caused an increase in S_b, which was in the range 2 to 58 mg · L^{-1}. Thus the ratio S_b/C_b is in the range 1–58, and one would expect S_b to be sensitive to changes in C_b caused by changing from pure oxygen to air. Tang and Fan (1987) employed C_b from 5.8 to 8.4 mg · L^{-1} and S_b from 2.69 to 6.49 mg · L^{-1}, and noted that in their work the degradation rate was independent of C_b. Thus S_b/C_b was in the range 0.32 to 1.0 and S_b would be expected to be largely unaffected by changes in C_b. Thus the critical ratio of S_b/C_b for transition determined in this work can be successfully used to explain the differing findings of other workers regarding the effect of dissolved oxygen concentration on the phenol degradation rate.

Conclusions

Microorganisms immobilized onto Celite diatomaceous earth particles were used to study phenol biodegradation in a draft-tube, three-phase fluidized-bed reactor.

In the absence of any correlations specifically obtained using a draft-tube FBR, correlations determined in a conventional FBR may be used to predict the liquid-solid mass transfer coefficients in a draft-tube FBR system. The error between k_e calculated from a correlation for conventional FBR's and k_e determined experimentally in this work was found to be approximately 20%. The Biot number for phenol was found to lie in the range 2–34. In four out of five runs, the phenol concentration at the surface of the biofilm was found to be less than 70% of the concentration in the bulk liquid. Thus it would seem that for this system the mass transfer coefficient is an important parameter and should not be overlooked.

The biofilms grown in this work exhibited a high density, which led to hindered diffusivity of oxygen and phenol within the biofilm. D_f/D_w decreased from 0.88 to 0.05 as the biofilm density increased from 141 to 217 kg · m^{-3}. This trend has been observed in other work. The effectiveness factor describing the diffusion and reaction of phenol in the biofilm decreased from 0.48 to 0.18 as the biofilm density increased from 141 to 217 kg · kg^{-1}. This decrease is attributable to decreasing diffusivity at higher biofilm densities.

A transition from oxygen-limited to phenol limited biofilm

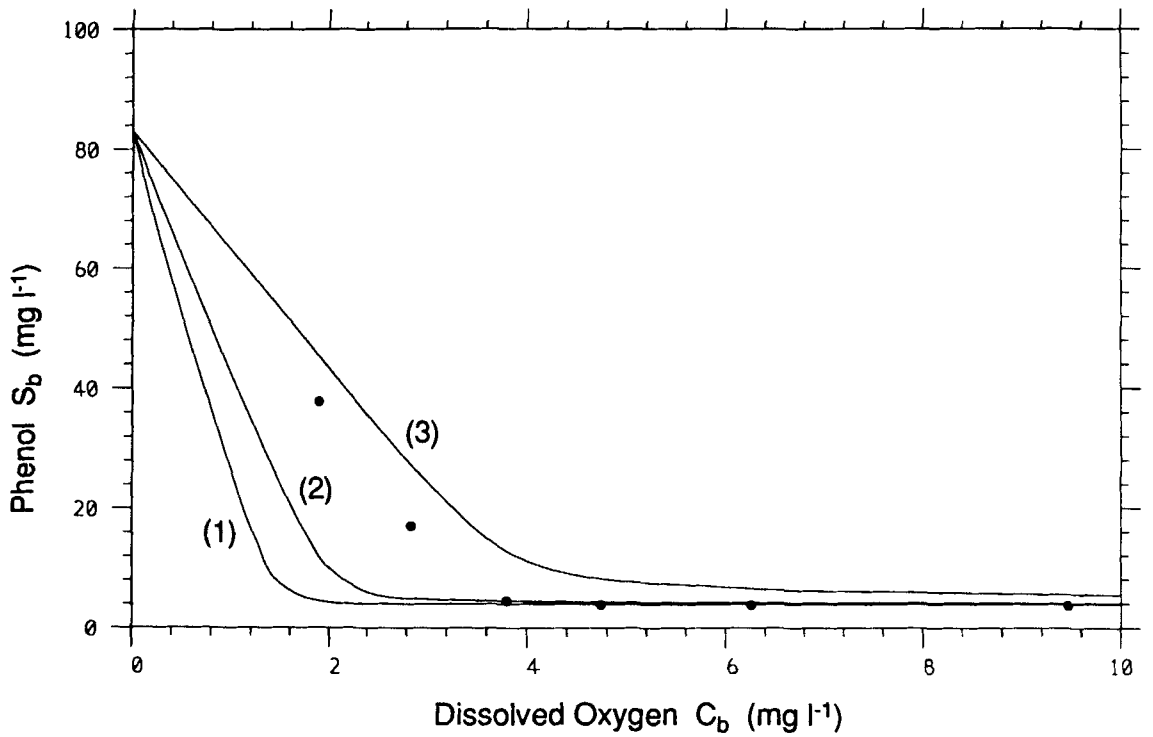

Figure 7. Effect of the Monod constant for oxygen on the transition from oxygen limited to phenol limited biofilm kinetics.

Phenol loading rate, $Q \cdot S_f = 0.78 \times 10^{-7}$ kg · s^{-1}; (●) experimental data (——) theoretical curves calculated with parameters in Table 5 except for K_o which is as follows: (1) 0.1×10^{-3} kg · m^{-3}; (2) 1.0×10^{-3} kg · m^{-3}; (3) 10.0×10^{-3} kg · m^{-3}

kinetics was found to occur experimentally when the ratio of phenol concentration to oxygen concentration in the bulk liquid, S_b/C_b, was in the range 0.9–1.1. The mathematical model proposed to describe the steady-state biofilm behavior predicts this transition reasonably well. Varying the assumed Monod kinetic constant for oxygen leads to even better agreement, and more experimental work is necessary to determine the actual value of this constant. This experimentally-determined transition between phenol-limiting and oxygen-limiting kinetics demonstrates the validity of the dual-substrate-limiting kinetic expression employed. It further explains the apparently differing findings of other workers regarding the effect of the dissolved oxygen concentration on the phenol degradation rate.

The significance of the critical ratio for the limiting substrate transition lies in its application to the economics of aerobic bioreactions. The cost of aeration may be significant in such an operation. The existence of this critical ratio implies that there is a point beyond which there is no return in volumetric reaction rate to be realized from investing in further aeration. A mathematical model such as the one used in this work can aid in evaluating where the most economic operating regions lie.

Notation

a = volumetric interfacial area of ion exchange beads, m^2/m^3
Bi_o = dimensionless group, $k_o \delta/D_{of}$
Bi_s = dimensionless group, $k_s \delta/D_{sf}$
c = ionic concentration, mol · L^{-1}
c_o = initial ionic concentration, mol · L^{-1}
c_i = ionic concentration at resin surface, mol · L^{-1}
C = dissolved oxygen concentration in biofilm, kg · m^{-3}
C_b = dissolved oxygen concentration in the bulk liquid phase, kg · m^{-3}
C_i = dissolved oxygen concentration at the interface between a bioparticle and the bulk liquid, kg · m^{-3}
C^* = dimensionless dissolved oxygen concentration, C/C_b
d_p = diameter of ion exchange bead, m
D = diffusion coefficient, $m^2 \cdot s^{-1}$
D_e = diffusion coefficient of ion in free solution, $m^2 \cdot s^{-1}$
D_f = diffusion coefficient in biofilm, $m^2 \cdot s^{-1}$
D_i = diffusion coefficient within ion exchange resin, $m^2 \cdot s^{-1}$
D_{of} = diffusion coefficient of oxygen in biofilm, $m^2 \cdot s^{-1}$
D_{ow} = diffusion coefficient of oxygen in water, $m^2 \cdot s^{-1}$
D_{sf} = diffusion coefficient of phenol in biofilm, $m^2 \cdot s^{-1}$
D_{sw} = diffusion coefficient of oxygen in water, $m^2 \cdot s^{-1}$
D_w = diffusion coefficient in pure water, $m^2 \cdot s^{-1}$
D_1, D_2 = diffusion coefficient of ionic species 1 or 2, $m^2 \cdot s^{-1}$
D_{12} = interdiffusion coefficient
g = acceleration due to gravity, m · s^{-2}
k = mass transfer coefficient, m · s^{-1}
k_e = liquid-solid mass transfer coefficient for ion exchange, m · s^{-1}
k_o = liquid-solid mass transfer coefficient for oxygen, m · s^{-1}
k_s = liquid-solid mass transfer coefficient for phenol, m · s^{-1}
K_{ba} = partition coefficient for ion exchange resin
K_i = inhibition constant for phenol, kg · m^{-3}
K_o = monod constant for oxygen, kg · m^{-3}
K_s = monod constant for phenol, kg · m^{-3}
K_i^* = dimensionless inhibition constant for phenol, S_b/K_i
K_o^* = dimensionless Monod constant for oxygen, K_o/C_b
K_s^* = dimensionless Monod constant for phenol, K_s/S_b
L = biomass loading, kg · kg^{-1}
m_p = mass of a single biomass-free bioparticle, kg
N_p = number of bioparticles in FBR
Q = flow rate of synthetic waste, $m^3 \cdot s^{-1}$
r = radial coordinate in biofilm, m
r_p = radius of biomass-free Celite particle, m
R_{obs} = observed rate of phenol removal in the reactor, kg · s^{-1}
R_{calc} = calculated rate of phenol removal in the reactor, kg · s^{-1}
S = phenol concentration in biofilm, kg · m^{-3}
S_b = phenol concentration in the bulk liquid, kg · m^{-3}
S_I = phenol concentration in inlet synthetic wastewater, kg · m^{-3}
S_i = phenol concentration at the interface between a bioparticle and the bulk liquid, kg · m^{-3}
S^* = dimensionless phenol concentration, S/S_b
Sc = Schmidt number, v/D
Sh = Sherwood number, $k\,d/D$
t = time, s
u_g = superficial gas velocity, m · s^{-1}
W = total biomass in reactor, kg
x = dimensionless distance, $r/r_p/\delta$
X = concentration of ion exchange groups in resin beads, mol · L^{-1}
Y_o/s = yield coefficient, kg oxygen · kg $phenol^{-1}$
Y_x/s = yield coefficient, kg biomass · kg $phenol^{-1}$
Y_x/o = yield coefficient, kg biomass kg $oxygen^{-1}$

Greek Letters

α = dimensionless group for ion exchange
ϵ = specific energy dissapation rate, $m^2 \cdot s^{-3}$
ϵ_p = particle volume fraction of ion exchange beads
δ = biofilm thickness, m
v = kinematic viscosity, $m^2 \cdot s^{-1}$
θ = effectiveness factor
ρ_v = biofilm density, kg · m^{-3}
μ = specific growth rate of biomass, s^{-1}, h^{-1}
μ_{max} = maximum specific growth rate of biomass, s^{-1}, h^{-1}
ϕ_o = dimensionless modulus for oxygen
ϕ_s = dimensionless modulus for phenol
λ = stagnant film thickness in ion exchange, m

Literature Cited

Andrews, G. F., and Chi-Tien, "Bacterial Film Growth in Adsorbent Surfaces," *AIChE J.*, **27,** 396 (1981).

Arters, D. C., and L.-S. Fan, "Solid Liquid Mass Transfer in a Gas-Liquid-Solid Fluidized Bed," *Chem. Eng. Sci.* **41,** 107 (1986).

Atkins, P. W., *Physical Chemistry,* 3rd ed., Oxford University Press, Oxford (1986).

Atkinson, B., and Mavituna, F., *Handbook of Biochemical Engineering,* Macmillan, London (1983).

Baker, E. E., R. J. Prevoznak, S. W. Drew, and B. C. Buckland, "Thienamycin Production by Streptomyces cattleya Cells Immobilized in Celite Beads," *Dev. Ind. Microbiol.*, **24,** 467 (1984).

Bauman, W. C., and J. Eichhorn, "Fundamental Properties of a Synthetic Cation Exchanger," *J. Amer. Chem. Soc.*, **69,** 2830 (1947).

Caunt, P., and H. A. Chase, "Biodegradation by Bacteria Immobilised on Celite Particles," *Bio/Technol.*, **6,** 721 (1988).

Denac, M., and I. J. Dunn, "Packed- and Fluidized-Bed Biofilm Reactor Performance for Anaerobic Wastewater Treatment," *Biotechnol. Bioeng.*, **32,** 159 (1986).

Donaldson, T. L., G. W. Strandberg, J. D. Hewitt, G. W. Shields, R. M. Worden, "Bioxidation of Coal Gasification Wastewaters Using Fluidized Bed Bioreactors," *Environ. Prog.*, **6**(4), 205 (1987).

Fan, L.-S., K. Fuije, T.-R. Long, and W. T. Tang, "Characteristics of Draft Tube Gas-Liquid-Solid Fluidized-Bed Bioreactor with Immobilized Living Cells for Phenol Degradation," *Biotechnol. Bioeng.*, **30,** 498 (1987).

Finlayson, B. A., *Nonlinear Analysis in Chemical Engineering,* McGraw-Hill, New York (1980).

Helfferich, F., *Ion Exchange,* McGraw-Hill, New York (1962).

Hill, G. A., and C. W. Robinson, "Substrate Inhibition Kinetics: Phenol Degradation by Pseudomonas Putida," *Biotechnol. Bioeng.*, **17,** 1599 (1975).

Holladay, D. W., C. W. Hancher, C. D. Scott, and D. D. Chilcote, "Biodegradation of phenolic waste liquors in stirred-tank, packed-bed, and fluidized bed bioreactors," *J. Water Poll. Control Fed.*, **50,** 2573 (1978).

Klein, J., U. Hackel, and F. Wagner, "Phenol Degradation by Candida tropicalis Whole Cells Entrapped in Polymeric Ionic Networks," *Immobilized Microbial Cells, ACS Symp. Ser., No. 106,* Amer. Chem. Soc., Washington, DC (1979).

Lapple, C. E., and C. B. Sheppard, "Calculation of Particle Trajectories," *Ind. & Eng. Chem.*, **32,** 605 (1940).

Libicki, S. B., P. M. Salmon, and C. R. Robertson, "The Effective Diffusive Permeability of a Nonreacting Solute in Microbial Cell Aggregates," *Biotech. Bioeng.*, **32,** 68 (1988).
Park, Y., M. E. Davis, D. A. Wallis, "Analysis of a Continuous, Aerobic, Fixed-Film Bioreactor: 1. Steady State Behaviour," *Biotech. Bioeng.*, **26,** 457 (1984).
Parkin, G. F., and R. E. Spence, "Anaerobic Biological Waste Treatment," *Chem. Eng. Prog.*, 55 (Dec., 1984).
Pawlowsky, U., and J. A. Howell, "Mixed Culture Bioxidation of Phenol: I. Determination of Kinetic Parameters," *Biotech. Bioeng.* **15,** 889 (1973).
Perry, R. H., and D. W. Green, *Chemical Engineers Handbook,* 6th ed., McGraw-Hill, New York (1984).
Powell, M. J. D., "A Hybrid Method for Nonlinear Equations," *Numerical Methods for Nonlinear Equations,* P. Rabinowitz, ed., Gordon and Breach, London (1970).
Robinson, D. K., and D. I. C. Wang, "Immobilized Cell Production of Xanthum Gum," ACS Meeting, Chicago (Sept. 9, 1985).
Sanger, P., and W. D. Dewcker, "Liquid-Solid Mass Transfer in Aerated Suspensions," *Chem. Eng. J.,* **22,** 179 (1981).
Tang, W.-T., and L.-S. Fan, "Steady State Phenol Degradation in a Draft Tube, Gas-Liquid-Solid Fluidized Bed Bioreactor," *AIChE J.,* **33,** 239 (1987).
Tang, W.-T., K. Wisecarver, and L.-S. Fan, "Dynamics of a Draft Tube Gas-Liquid-Solid Fluidized Bed Bioreactor for Phenol Degradation," *Chem. Eng. Sci.,* **42,** 2123 (1987).
Villadsen, J., and M. L. Michelson, *Solution of Differential Equation Models by Polynomial Aproximation,* Prentice Hall, Englewood Cliffs, NJ (1978).
Wagner, K., and D. C. Hempel, "Biodegradation by Immobilized Bacteria in an Airlift-Loop Reactor—Influence of Biofilm Diffusion Limitation," *Biotech. Bioeng.*, **31,** 559 (1988).
Wang, D. I. C., J. Meier, and K. Yokoyama, "Penicillin Fermentation in a 200-Liter Tower Fermenter Using Cells Confined to Microbeads," *Appl. Biochem. Biotechnol.*, **9,** 105 (1984).
Wang, S.-C. P., and Chi-Tien, "Bilayer Film Model for the Interaction Between Adsorption and Bacterial Activity in Granular Activated Carbon Columns," *AIChE J.*, **30,** 786 (1984).
Washburn, E. W., *International Critical Tables,* McGraw-Hill, New York (1926).
Worden, R. M., and T. L. Donaldson, "Dynamics of a Biological Fixed Film for Phenol Degradation in a Fluidized-Bed Bioreactor," *Biotech. Bioeng.*, **30,** 398 (1987).
Yang, R. D., and A. E. Humphrey, "Dynamic and Steady State Studies of Phenol Biodegradation in Pure and Mixed Cultures," *Biotech. Bioeng.*, **17,**1211 (1975).

Manuscript received May 30, 1989, and revision received Sept. 26, 1989.